POAC'23
Glasgow, United Kingdom

Proceedings of the 27th International Conference on
Port and Ocean Engineering under Arctic Conditions
12-16 June 2023, Glasgow, United Kingdom

Velocity field and force distribution in an unconsolidated ice ridge penetrated by a ship

Hanyang Gong[1], Arttu Polojärvi[2], Jukka Tuhkuri[2]
[1] Aker Arctic Technology Inc, Helsinki, Finland
[2] Aalto University, School of Engineering, Department of Mechanical Engineering, Espoo, Finland

ABSTRACT

Estimating ship resistance in ice ridges requires an understanding of ridge failure processes. A three-dimensional discrete element method is used to study a ship passing through a small unconsolidated ridge with a triangular cross-section and the resulting velocity field and force distribution inside the ridge. The kinetic behavior of ice blocks within the ridge suggests a gradual failure process, not a sudden failure. The velocity field shows fast-moving ice blocks near the ship bow, and stationary or slow-moving blocks further away. Loads within the ridge were transmitted through force chains. No unique shear planes were observed.

KEY WORDS: Ridge; Resistance; Force chain; Failure behavior.

INTRODUCTION

Ships operating in ice-covered waters often encounter pressure ridges. However, the ridge resistance has a minor role in ship design and our understanding of ridge resistance is limited. An ice ridge is typically divided into a sail, a keel, and a consolidated layer in between. In ridge resistance studies it is customary to study the resistance due to the ridge keel only, as its mass is often significant and behavior different from level ice. In this paper we use the term ridge resistance to refer to the ridge keel resistance.

Prediction of ridge resistance requires knowledge of the dimensions and material properties of ridges and understanding of their mechanical behavior under loading. Ridge keels have been modelled as continuum or discontinuous models. Early analytical models assumed a ridge failure through shear, similar to soil mechanics (Keinonen, 1979, Malmberg, 1983). Both the models converted the three-dimensional problem into a two-dimensional one and considered the ice rubble was passively resisted the ship by applying the Rankine theory. Such models assume a failure through a shear plane, but ice ridges failing along distinct shear planes caused by ships have never been observed. Another approach is to use discontinuous models, such as

the discrete element method (DEM), to study the kinetic behavior of each ice block in a ridge (Gong et al., 2019, Gong, 2021). Such methods model the Newtonian dynamics of interacting ice blocks without a priori assumption of the failure mode or failure geometry and have shown that the ridge resistance is related to the ridge deformation represented by the mass of ice blocks accelerated by and moving with the ship.

This paper presents results from DEM simulations on the kinetic behavior of ice blocks inside a 5-m-deep unconsolidated ridge with a triangular cross-section and shows the velocity field and force distribution within the ridge when a simulated ship, MT Uikku, penetrated the ridge.

NUMERICAL SIMULATIONS

The study reported here is performed by using an in-house 3D DEM code developed by Aalto University Ice Mechanics Group. Detailed description of the code and its validation for modeling ice rubble are presented by Polojärvi and Tuhkuri (2009) and Polojärvi et al. (2012). We have earlier applied the code to simulate a ship passage through an ice ridge (Gong et al., 2017) and to study the effect of ridge width on ice ridge resistance (Gong et al., 2018). A reader can find a detailed description of the simulation setup from Gong (2021).

Figure 1a presents the simulation domain with the coordinate system used in the further text. A half model, the part where $y < 0$, was modelled, including the ship model and ice rubble forming the unconsolidated ridge keel. A horizontal plane at waterline at $z = 0$ constrains the ice ridge from dissolving, which is illustrated as "ice cover" (plane constraint) in Figure 1a. A ridge can be described by ridge depth h, width w and length l_f defined as shown in the figure. Constraining vertical plane at y = -30 m was far enough from the ship to not affect the ice rubble deformation process of the rubble (Gong et al., 2017).

The simulated ridge was unconsolidated and consisted of rigid cuboid-shaped blocks with a thickness h_{ice}. The other two dimensions of the blocks varied randomly but followed the shape distribution given by Kulyakhtin and Høyland (2014), with a restriction of aspect ratio. Main parameters used in the simulations are listed in Table 1.

Table 1. Parameters used in the simulation.

Description		Symbol	Unit	Value
Ridge	Depth	h	m	5
	Length	l_f	m	60
	Width	w	m	17.3
Ice block	Thickness	h_{ice}	m	0.3
	Aspect ratio	-	-	0.6...15
	Density	ρ_i	kg/m^3	920
	Ice-ice friction coefficient	μ_i	-	0.3
	Ship-ice friction coefficient	μ_s	-	0.1
Water	Density	ρ_ω	kg/m^3	1010
Ship	Velocity	v_{ship}	m/s	1

The simulated ice ridge was generated in two stages as described in detail in Gong (2021). The first stage involved releasing ice blocks having random initial velocities underwater in a simulation domain larger than the designated ridge dimensions. As the ice blocks floated upwards and their kinetic energy became dissipated, the ice rubble or ice pile was formed. On the second stage the ice blocks with all their vertices inside the designated ridge dimensions were chosen and used for further simulation. This ridge model generation allows the ridge to have a random initial configuration and porosity varying in the range of 0.4...0.5, which aligns with full-scale observations on ridge porosities (Høyland, 2007).

An ice-strengthened tanker MT Uikku was simulated. This modeled ship has a wedge-shaped bow common to ice-going ships. The bow form can be characterized by the following bow angles: waterline angle α, stem angle φ and flare angle ψ, as illustrated in Figure 1b. α =25.2°, φ=29.7°, and ψ=53.3° at B/4. L_{bow} = 20 m, L_b = 40 m, B = 22 m, and T = 9.5 m.

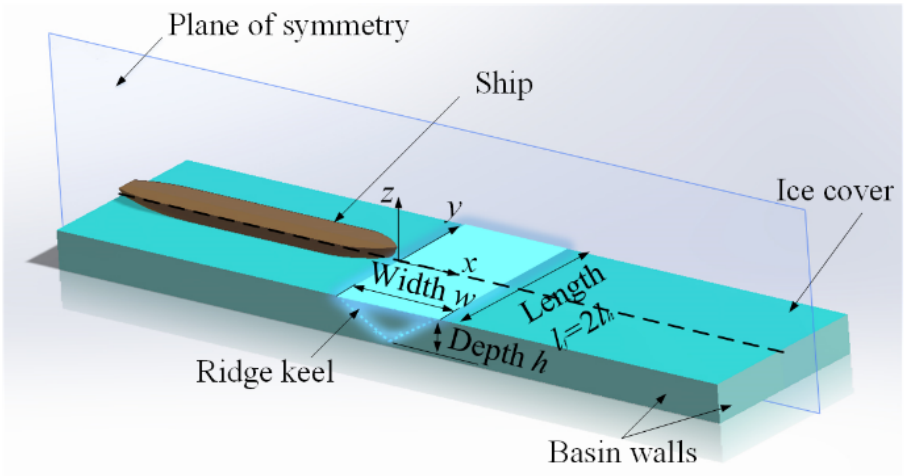

(a)

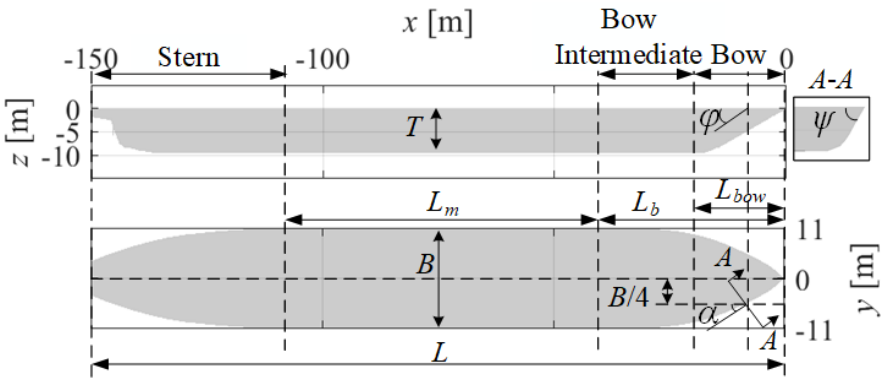

(b)

Figure 1. (a) The simulation domain and the coordinate system. w is ridge width, l_f is ridge length, and h is ridge depth. (b) MT Uikku's hull dimensions and three bow angles.

AVERAGE STRESS

A direct output of DEM simulations are forces applied on individual ice blocks. These can be

used to derive an average stress tensor for each block, calculated as described in, for example, Bagi (1996). The stress tensor is defined as

$$\sigma^p = \bar{\sigma}_{ij} = \frac{1}{V^P}\sum_{C=1}^{N_c} f_i^c \, r_j^c, \quad (1)$$

where N_c is the number of contacts on a block p, V^P is the volume of the block, and f_i^c is the contact force. The unit branch vector r_j^c has the direction of a vector from the centroid of the block to the point of contact of f_i^c. The subscripts i and j correspond to the x-, y-, z-axis. The stress tensor can be decomposed as

$$\sigma^p = \sigma = \sigma_{sym} + \sigma_{skew} \quad (2)$$

into a symmetric and a skew part, $\sigma_{sym} = \frac{1}{2}(\sigma + \sigma^T)$ and $\sigma_{skew} = \frac{1}{2}(\sigma - \sigma^T)$, respectively. Symmetric part σ_{sym} represents Cauchy stress (Rothenburg and Bathurst, 1989) with the hydrostatic pressure given by

$$\sigma_h = \frac{1}{3}\sum_{ii=1}^{ii=3} \sigma_{ii,sym} \quad (3)$$

that can be interpreted as the average normal stress within a block. In brief, when σ_h is high, the block is under high compression due to contact forces applied on it. Below σ_h is used to illustrate force chains, sequences of contacting blocks under high compressive stresses.

RIDGE RESISTANCE

Figure 2 shows the calculated ridge resistance (R) as a function of the horizontal displacement (δ) of the ship. $\delta = 0$ m when the ship bow enters the ridge and R is the x-component of the sum of all the contact forces on the ship. The simulation validation can be found in Gong (2021). The $R - \delta$ record shows different stages. As the ship penetrates the ridge, R increases with δ to a peak value R^p, and when the bow starts to exit the ridge, R starts to decrease. The resistance is constant when only the ship midbody is in contact with the ridge and gradually decreases to zero when the ship exits the ridge. The shape of the $R - \delta$ record depends on dimensions of both the ship and the ridge.

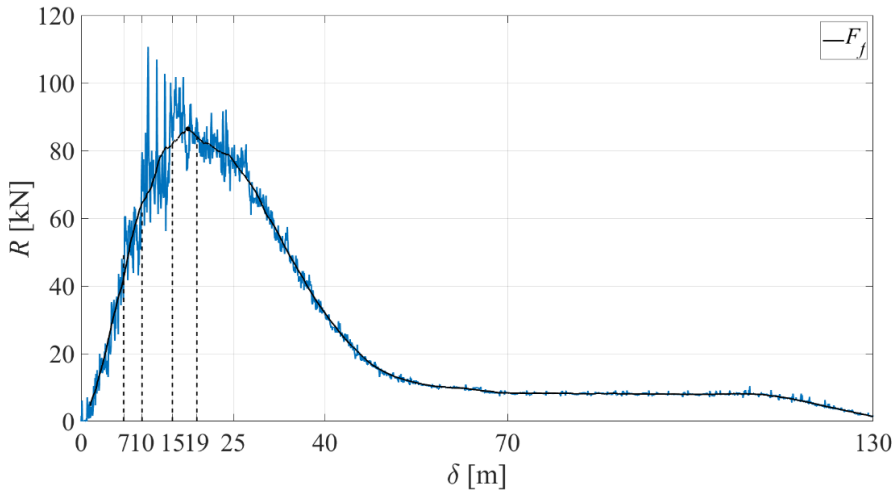

Figure 2. Ridge resistance record $R - \delta$ for the ridge shown in Figure 1a. A running average F_f with a window size of 6 m is shown as a black line. The displacements 7 m, 10 m, 15 m, and 19 m refer to events analysed below in detail.

VELOCITY FIELD AND FORCE DISTRIBUTION WITHIN A RIDGE

Figure 3 shows the velocity field projected onto the *xy*-plane (z=0) within the ridge at four time-instants. The block velocities are shown relative to the ship's velocity. At δ = 7 m, only the ice blocks near the bow are accelerated by the ship and are moving on trajectories normal to the ship hull at the bow. At δ = 10 m, a larger volume of ice blocks is moving, and the resistance is higher. At this stage ice blocks at the far end of the ridge start to move, which leads to a decrease in the slope of the $R - \delta$ record, reflecting the disintegration of the ridge. At δ = 15 m, the ship is reaching the far end of the ridge, and as the ridge is disintegrating, the ice blocks are moving faster than during earlier stages of the interaction. At δ = 19 m, the ship bow is out of the ridge and the resistance starts to gradually decrease. In Figure 3 boundaries between moving and stationary ice blocks can be identified, but importantly, the locations of these boundaries change during the ship-ridge interaction, and no distinct shear line or shear zone can be observed.

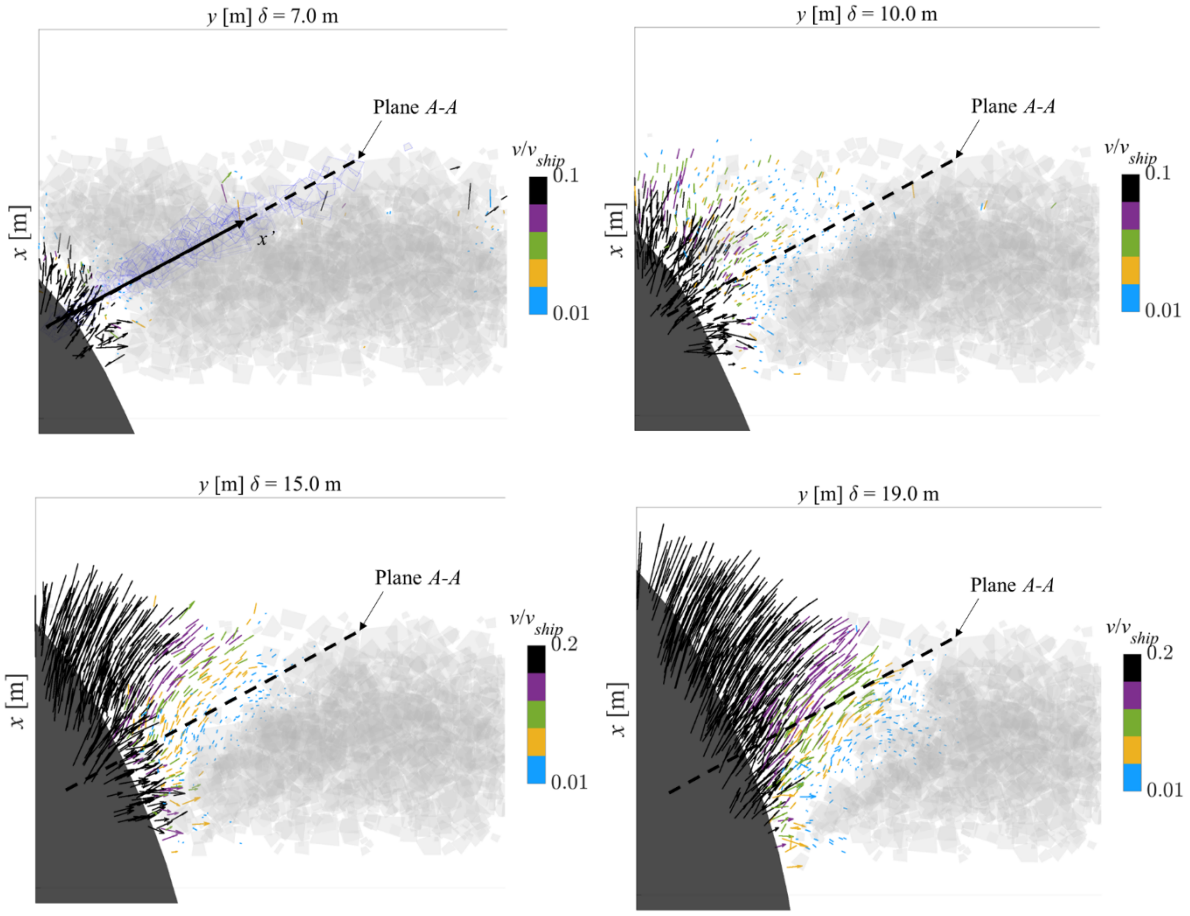

Figure 3. Velocity field of an entire ridge projected onto the *xy*-plane (z = 0) at δ of 7, 10, 15, and 19 m. The velocity vectors of blocks are coloured based on the colour bar of v normalised by v_{ship}. The dashed lines show the location of the vertical plane used in the analysis below. The blocks with blue edges illustrated at δ of 7 m are associated with the vertical plane studied in Figures 4 and 5. Grey blocks are stationary, for them $v < 0.01 v_{ship}$.

Figure 4 illustrates the velocity field within the ice ridge in a single vertical plane. This plane,

shown in Figure 1b as the plane *A-A*, is located where the ship is at δ = 15 m. Thus, the plane studied is not moving with the ship, but is defined to be normal to the ship hull at one time instant. The ice blocks associated with the plane were selected as follows: if the initial distance of the centroid of an ice block was equal or less than 2 m from the plane, the ice block was associated with the plane and the velocity of that block was traced.

The velocity field within the ridge, during the ship penetration, shows a gradient. Ice blocks are moving faster near the ship than further away. In addition, the velocity fields show how the ice blocks are accelerated and how the volume of the moving blocks is increasing by the approaching ship. At first, when δ = 7 m, the moving ice blocks move downwards to a direction of about 45° to the horizon. As the ship moves further into the ridge, the velocity vectors turn horizontal following the direction of the normal of the ship hull.

Figure 4 identifies three zones: fast moving ice blocks near the ship (black arrows), a transition zone (arrows other than black), and a far field with stationary blocks (grey ice blocks, no arrows). Defining v_f as the velocity of the fastest ice block, blocks with velocity more than $0.8v_f$ were considered fast, and blocks with velocity less than $0.8v_f$ were considered part of the transition zone. The transition zone had varying shapes during the ship's penetration into the ridge.

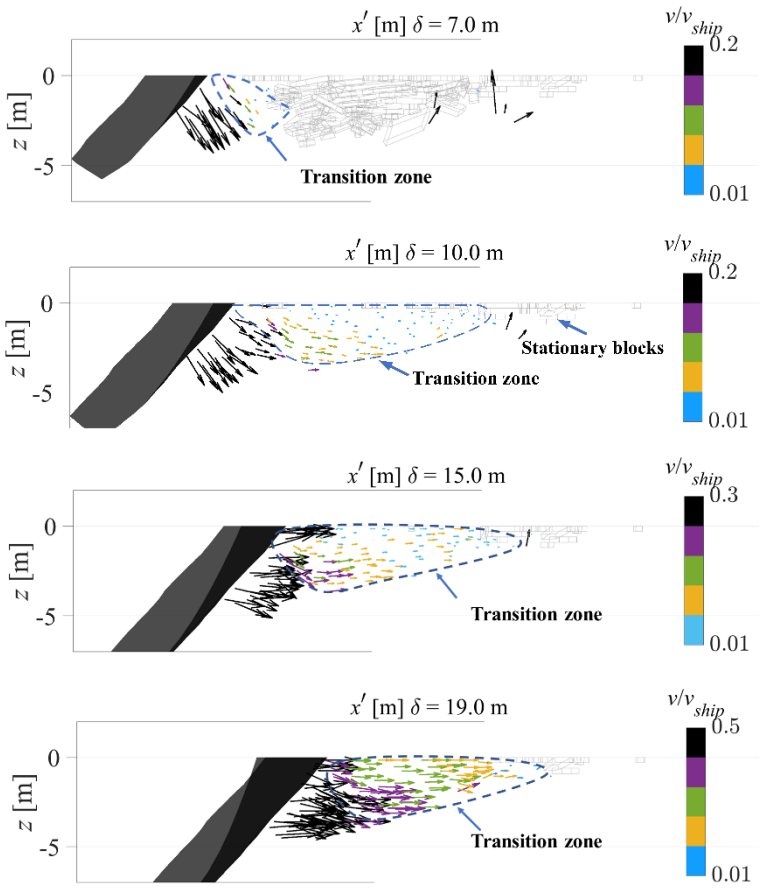

Figure 4. Velocity field of ice blocks in the ridge at vertical plane. The border of the transition zone is illustrated by a blue dashed contour. The *x'*-axis is illustrated in Figure 3 δ = 7 m.

Figure 5 shows the distributions of block-to-block forces within the ridge, in the same vertical plane as analysed above and defined in Figure 3. In the figure, blocks are coloured when σ_h

(Equation 3) is larger than the mean σ_h of all the blocks. At δ = 7 m, the contact loads concentrate on blocks near the bow and waterline. At δ = 15 m, when the ship is about to pass through the ridge, the highly stressed blocks form an arch-like pattern, bridging the blocks between the ship bow and the far-end of the ridge. These blocks resist the ship's penetration into the ridge. When the ship exits the ridge at δ = 19 m, the mean contact force shows a higher value than earlier.

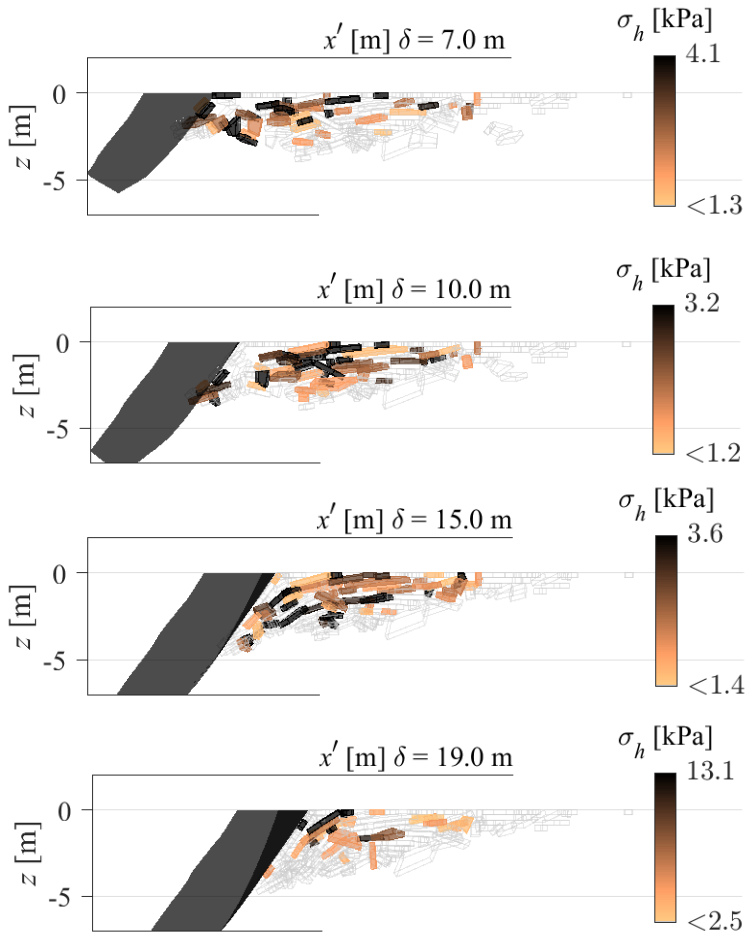

Figure 5. Block-to-block contact force distribution in the vertical plane defined in Figure 3.

CONCLUSION

The velocity fields and force distributions within a narrow ridge penetrated by MT Uikku were studied by using DEM simulations. The velocity fields show fast-moving ice blocks near the ship bow, and slow or stationary blocks further away. Loads within the rubble were transmitted through force chains having arch-like shapes.

The early analytical models on ridge resistance by Keinonen (1979) and Malmberg (1983), which are still occasionally used as new analytical models have not been developed, assume that a peak resistance is reached when a shear plane within the rubble is initiated. In the case studied here, the peak resistance was reached at about δ = 19 m, and the velocity field in Figure 4 shows that the whole rubble was moving at that stage. No distinct shear plane or shear zone

can be observed. This result is in line with studies on ridge punch-through tests (Polojärvi and Tuhkuri 2009). The ridge failure by a ship was observed to be a gradual process, where the ice blocks are accelerated by the ship, rather than a sudden shear failure occurring in the ridge material, as assumed in the analytical models.

ACKNOWLEDGEMENTS

The first author gratefully acknowledges financial support from K. Albin Johanssons stiftelse sr. The paper's content is part of the first author's doctoral thesis at Aalto University.

REFERENCES

Bagi, K., 1996. Stress and strain in granular assemblies. *Mechanics of materials*, 22, pp.165-177.

Gong, H., Polojärvi, A., & Tuhkuri, J., 2017. Preliminary 3D DEM simulations on ridge keel resistance on ships, *Proceedings of the 24th International Conference on Port and Ocean Engineering under Arctic Conditions, POAC'17*.

Gong, H., Polojärvi, A., & Tuhkuri, J., 2018. 3D DEM Study on the effect of ridge keel width on rubble resistance on ships, *Proceedings of the 37th International Conference on Ocean, Offshore and Arctic Engineering, ASME 2018*.

Gong, H., Polojärvi, A., & Tuhkuri, J., 2019. Discrete element simulation of the resistance of a ship in unconsolidated ridges. *Cold Regions Science and Technology*, 167, 102855.

Gong, H., 2021. *Discrete-element modelling of ship interaction with unconsolidated ice ridges: ridge resistance and failure behaviour*. Ph.D. Espoo: Aalto University.

Høyland, K. V., 2007. Morphology and small-scale strength of ridges in the North-western Barents Sea. *Cold Regions Science and Technology*, 48, pp. 169-187.

Keinonen, A., 1979. *An analytical method for calculating the pure ridge resistance encountered by ships in first year ice ridges*. Ph.D. Espoo: Helsinki University of Technology.

Kulyakhtin, S. & Høyland, K. V., 2014. Distribution of ice block sizes in sails of pressure ice ridges, *Proceedings of the 22nd IAHR International Symposium on Ice*.

Malmberg, S., 1983. *Om fartygs fastkilning i is*. Master. Espoo: Helsinki University of Technology.

Polojärvi, A. & Tuhkuri, J., 2009. 3D discrete numerical modelling of ridge keel punch through tests. *Cold Regions Science and Technology*, 56, pp.18-29.

Polojärvi, A., Tuhkuri, J., & Korkalo, O., 2012. Comparison and analysis of experimental and virtual laboratory scale punch through tests. *Cold Regions Science and Technology*, 81, pp. 11-25.

Rothenburg, L. & Bathurst, R. J., 1989. Analytical study of induced anisotropy in idealized granular materials. *Geotechnique*, 39, pp.601-614.